Self-Configuring Silicon-Photonic Receiver for Multimode Free Space Channels

SeyedMohammad SeyedinNavadeh(1), Maziyar Milanizadeh (1), Giorgia Benci(1), Christian De Vita(1), Charalambos Klitis(2), Marc Sorel(2), Francesco Zanetto(1), Vittorio Grimaldi(1), Giorgio Ferrari(1), David A.B. Miller(3), Andrea Melloni(1), Francesco Morichetti(1)

(1) Dipartimento di Elettronica, Informazione e Bioingegneria - Politecnico di Milano, Milano, 20133 Italy. (*maziyar.milanizadeh@polimi.it*)

(2) School of Engineering University of Glasgow, Glasgow, G12 8QQ, U.K

(3) Ginzton Laboratory, Stanford University, Spilker Building, Stanford, CA 94305, USA

***Abstract*—A self-configuring mesh of silicon Mach-Zehnder Interferometers is employed to receive two spatially overlapped orthogonal beams modulated at 10 Gbit/s. These beams, sharing the same wavelength and state of polarization, are separated with more than 30 dB isolation, and sorted out with no signal degradation.**

Keywords*— *free space optics, silicon photonics, programmable photonic processors

I. Introduction

Programmable Photonic Integrated Circuits (PICs) consisting of feed-forward or recursive meshes of tunable optical interferometers are rapidly emerging as versatile architectures in many different fields of application [1], including microwave photonics [2], imaging and beam shaping [3], and quantum [4] and neural networks [5]. In particular, the capability of performing arbitrary linear transformations make these devices attractive for applications requiring advanced manipulation of orthogonal optical modes. In a previous contribution, we demonstrated that a silicon photonic mesh of Mach-Zehnder Interferometers (MZIs) can automatically perform unmixing and sorting of guided modes that are mixed by propagation in a multimode waveguide [6]. In this work, we show that the same architecture can be used as a receiver for multimode free space channels. Two spatially overlapped Hermite-Gaussian (HG) beams modulated at 10 Gbit/s and sharing the same wavelength and State of Polarization (SOP) are separated and sorted out by the receiver without introducing any excess loss or degradation in the quality of the transmitted signals.

II. Photonic Circuit Structure

The circuit consists of a mesh of MZIs in a 9x2 diagonal configuration with two rows of 8 and 7 MZIs (Fig.1a), respectively, which terminates at one end with a square 3x3 optical antenna array of vertically emitting grating couplers. This array is exploited to either couple free space beams into the photonic chip or to radiate guided modes out to free space. The fabricated chip (Fig.1b) is fabricated on a standard 220 nm silicon photonic platform (AMF foundry), making use of 500 nm-wide channel waveguides. The optical antennas of the array (grating couplers) are placed 50 μm apart from each other in a square configuration. Each balanced MZI in the mesh has an arm length of 80 μm and a width of 70 μm, and integrates two 3 dB directional couplers with 40 μm width and 300 nm gap. The amplitude and phase tunability of each MZI is enabled making use of two thermo-optic actuators (heaters) made of TiN metal strips, fabricated on top of the waveguides in internal and external arms of the MZI. The working point of each MZI can be controlled exploiting the transparent CLIPP photodetectors [7], which are fabricated on one of the output ports of each MZI of the mesh. Making use of the required electronic front-end, the automated control algorithm can be implemented through reading-out of the CLIPP detectors and providing proper control signals to the thermal phase-shifters.

III. Sorting Out Overlapping Modes

This PIC is exploited for separating and sorting out two spatially overlapped free-space orthogonal optical beams, thus implementing a receiver for Mode Division Multiplexing (MDM) free space optical communications links. Fig.1(c) shows a schematic of the optical setup. The same setup can be used in a "forward" direction to couple two overlapped optical beams co-propagating from two different fiber collimators (Free Space optical Transmitters, FS-TXs) into the photonic chip (Photonic Integrated Receiver, PI-RX), or in a "reverse" direction to radiate two different, overlapping beams from the Photonic Integrated Transmitter (PI-TX) to the two Free Space Receivers (FS-RXs). Considering for simplicity the second case, a tilted mirror is positioned above the optical antenna array of the PI-TX to steer the direction of propagation of the vertically radiating grating couplers to the horizontal direction. A bi-convex lens with focal length of f_1 = 50 mm is placed in front of the chip in a Fourier transforming condition to obtain a collimated far-field of the radiated beam at plane P1. Another lens with the same focal length f_1 is used to image the plane of the array at plane P2 (4f imaging system). The third bi-convex lens with focal length f_2 = 75 mm creates a collimated far-field beam matched to the aperture of the FS-RXs. A 50/50 cube beam-splitter is used to split the beam in two optical paths and the beam size at the center of the beam-splitter is one-to-one imaged at the planes where the FS-RXs are placed by means of two bi-convex lenses with focal length f_3 = 250 mm.

When shining two orthogonal beams from the FS-TXs (namely FS-TX1 and FS-TX2) to the PI-RX, the mesh of MZIs can be configured in such a way that the two orthogonal beams are directed to two different output single-mode waveguides (WG1 and WG2, Fig.1a). In the experiment reported in Fig. 1, we consider the case where FS-TX1 transmits the fundamental symmetric HG00 mode, whereas a phase mask is placed in front of FS-TX2 (Fig.1c), in order to generate an "antisymmetric" (and therefore orthogonal) mode, approximately like the higher-order HG01 mode (from here on HG01). The two beams share the same wavelength (1550 nm) and horizontal polarization (matching the TE mode of the grating couplers), and impinge spatially overlapped on the optical antenna array of the PI-RX. The two rows of MZIs automatically line up by minimizing the optical power at

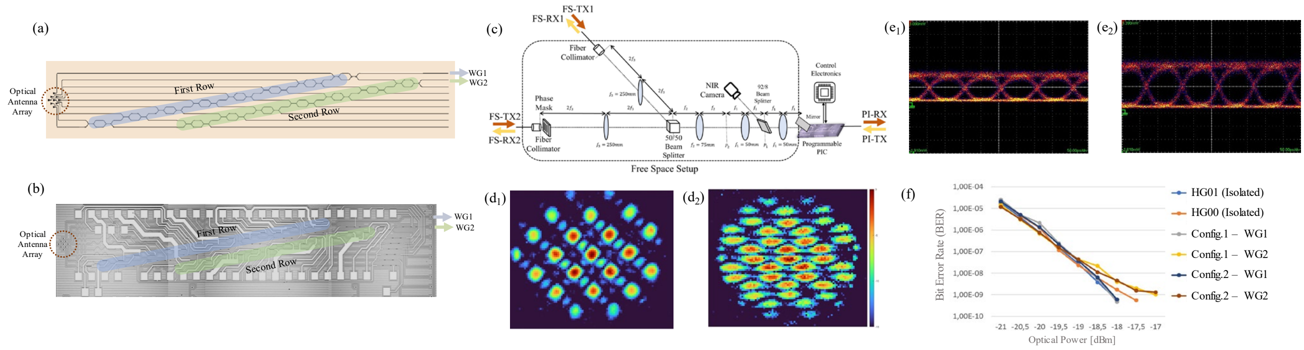

Figure 1: (a) A simplified schematic of the 9×2 diagonal mesh of MZIs including 9 optical waveguides connected to a 3x3 optical antenna array placed on the left and two waveguide ports (WG1 and WG2) on the right. The two MZI rows allow for reconstruction and sorting of two orthogonal free space modes coupled through optical antenna array at the WG ports; (b) Microscopic image of the fabricated silicon PIC; (c) Schematic of the experimental setup; (d) Radiated far-field beam of the mesh captured via a near- IR camera in case of being tuned to the fundamental HG00 mode (d_1) and higher-order HG01-like mode (d_2); (e) Eye diagrams recorded for 10 Gbit/s OOK modulated signal extracted at WG1 (e_1) and WG2 (e_2) coming from FS-TX1 (HG00 mode) and FS-TX2 (HG01-like mode), respectively. (f) BER measured for the received channels after reconstruction and sorting at the two output WG ports of the PI-RX.

lower output port of each MZI in a row, independently from each other, by applying proper phase shifts and monitoring the power on the integrated detectors [6]. Results show that the two beams are reconstructed, separated and sorted out at the output WG ports with more than 30 dB mutual isolation.

Once the mesh is tuned and the incoming free space beams are coupled to the two output waveguides, the direction of the light propagation can be reversed (from PI-TX to FS-RXs) in order to analyze the radiation pattern of the optical antenna array. The field radiated by the PI-TX is acquired by a near-IR camera, focused at plane P1 using a 92/8 beam- splitter (Fig.1.a). Since the radiating elements of the optical antenna array are several wavelengths apart (~32λ), a number of diffraction orders (grating lobes) are present in the radiation pattern, with the orders spaced ~ 1.7 degrees apart. Each one of these higher diffraction orders contains an approximate replica of the "central" spot. (Such diffraction effects could be reduced by, for example, using an array of lenslets above the grating couplers.) As an example, Figs. 1d_1 and 1d_2 show the far-field pattern radiated by the mesh when the light is injected to WG1 and WG2, respectively, demonstrating, in each "spot", a good match with the shape of the fundamental HG00 mode and the higher-order HG01 mode.

The quality of the reconstructed beam in each "spot" is limited by the number of grating couplers in the optical antenna array, providing the sampling pixels of the discretized modes manipulated by the mesh. Although in our case we work with only 9 pixels, transmission experiments demonstrate that orthogonality is well preserved and the realized PIC can be used for MDM free space channels. The two free space optical beams transmitted by the FS-TXs at 1550 nm are modulated at 10 Gbit/s OOK and the MZI rows of the mesh are tuned to extract the HG00 mode and the HG01 at the two output ports WG1 and WG2. The quality of the received signals can be appreciated in Fig. 1e_1 and 1e_2, showing clearly open eyes with no evidence of coherent crosstalk. To quantify the effect of the residual interfering channel, we measured the Bit Error Rate (BER) versus optical power at the receiver for both signals (modes) sorted at different output ports (Fig.1f). As a reference curve, we measured the BER for the two individual modes HG00 only (red) and HG01 only (light blue) – that is, when the interfering mode is turned off. The other curves show the BER of the extracted channels at output ports WG1 and WG2 of the mesh for different sorting configurations (Config.1: HG00 to WG1, "HG01" to WG2; and Config.2: "HG01" to WG1, HG00 to WG2). Overlapping of all the BER curves demonstrates that the two signals are well reconstructed with high mutual isolation between the received modes.

IV. Conclusions

We demonstrated that a silicon photonic mesh of MZIs effectively separates overlapped free space channels sharing the same wavelength and SOP and can be used as a receiver for MDM free space optical communications. More than 30 dB isolation is achieved on a pair of overlapped Hermite-Gaussian-like beams modulated at 10 Gbit/s, resulting in negligible penalties in the quality of the transmitted signals. Applications can be expanded to more advanced MDM schemes, all-optical signal processing, phase-front reconstruction, and automatic establishment of free space optimal communication links [8].

Acknowledgment

This work was supported by the European Commission through the H2020 project SuperPixels (grant 829116). DM acknowledges support from AFOSR under award number FA9550-17-1-0002. Part of this work was carried out at Polifab, Politecnico di Milano, Milan, Italy.

References

[1] W. Bogaerts, et al. "Programmable photonic circuits". Nature 586, 207–216 (2020). https://doi.org/10.1038/s41586-020-2764-0

[2] D. Pérez, et al., "Toward Programmable Microwave Photonics Processors," J. Lightwave Technol. 36, 519-532 (2018)

[3] M. Milanizadeh, et. al. "Automated manipulation of free space optical beams with integrated silicon photonic meshes," arXiv:2104.08174

[4] X. Qiang, et al., "Large-scale silicon quantum photonics implementing arbitrary two-qubit processing," Nat. Photonic, vol. 12, pp. 534–539 (2018)

[5] Y. Shen et al., "Deep learning with coherent nanophotonic circuits," Nat. Photonics, vol. 11, pp, 441–446 (2017)

[6] A. Annoni, et al. "Unscrambling light—automatically undoing strong mixing between modes". Light: Science & Applications 6, e17110 (2017).

[7] F. Morichetti, et al, "Non-invasive on-chip light observation by contactless waveguide conductivity monitoring," J. Selected Topics in Quantum Electronics, vol. 20, no. 4, Jul./Aug. 2014.

[8] D. A. B. Miller, "Establishing Optimal Wave Communication Channels Automatically," J. Lightwave Technol. 31, 3987-3994 (2013)